

Extended release of highly water soluble isoniazid attained through cocrystallization with curcumin

Bianfei Xuan¹, Si Nga Wong¹, Yanjie Zhang^{1,2}, Jingwen Weng¹, Henry H.Y. Tong³, Chenguang Wang⁴, Changquan Calvin Sun⁴, Shing Fung Chow^{1,*}

¹Department of Pharmacology and Pharmacy, Li Ka Shing Faculty of Medicine, The University of Hong Kong, Pokfulam, Hong Kong SAR, China

²Ocean College, Minjiang University, Fuzhou, Fujian, 350108, China

³School of Health Sciences, Macao Polytechnic Institute, Macao SAR, China

⁴Pharmaceutical Materials Science and Engineering Laboratory, Department of Pharmaceutics, College of Pharmacy, University of Minnesota, USA

** Corresponding author*

Shing Fung Chow

Department of Pharmacology and Pharmacy

Li Ka Shing Faculty of Medicine

The University of Hong Kong

L2-08B, Laboratory Block,

21 Sassoon Road, Pokfulam, Hong Kong

Email: asfchow@hku.hk

Tel: +852-39179026

Fax: +852-28170859

ABSTRACT: The aim of this study was to design and evaluate a cocrystal capable of releasing a highly water soluble drug, isoniazid (INH), over a period of longer than several hours by forming a cocrystal with curcumin (CUR). The 2:1 INH-CUR cocrystal can not only lower the dissolution rate of INH but also exhibit potential therapeutic synergy. A phase pure INH-CUR cocrystal was obtained by rapid solvent removal above a threshold evaporation rate. The formation of INH-CUR cocrystal was confirmed by powder X-ray diffraction and the construction of a temperature-composition phase diagram with differential scanning calorimetry. The pharmaceutical properties of the INH-CUR cocrystal, including hygroscopicity, stability and dissolution performance, were compared to those of INH and CUR. Extended release of INH from the cocrystal was observed in both pH 1.2 and pH 6.8 buffers, while their release patterns behaved differently. The dissolution kinetic of INH-CUR cocrystal followed Fickian diffusion and was controlled by the cocrystal solubility and the mode of CUR recrystallization. At pH 1.2, a significant amount of CUR form III precipitated and recrystallized onto the surface of undissolved cocrystals after 4 h, and thus substantially inhibited the INH release from cocrystal thereafter. On the other hand, ~90% INH was released linearly at pH 6.8 in the first 18 h, and complete release of INH was attained at 24 h. This work demonstrated that cocrystallization is a promising formulation strategy for achieving up to 48 h of drug release without using polymers.

Keywords: cocrystal, extended release, curcumin, isoniazid, drug dissolution

1. Introduction

Extended release dosage forms are designed to maintain therapeutic levels of drugs in a controlled manner over an extended period of time.¹ They possess several advantages, such as reducing dosing frequency, local and systemic adverse effects by minimizing drug plasma level fluctuation.² A number of formulation strategies are available for achieving extended release profiles, including the use of polymeric matrices, membrane-controlled systems, and osmotic pumps.³ However, these systems are often associated with issues in drug loading efficiency⁴ and instability.⁵ Formulating extended release dosage forms of highly water soluble drugs without polymers is particularly hard to achieve because of the inherently faster dissolution of soluble solid form.⁶ Cocrystallization is an approach capable of altering solubility and dissolution performance of an active pharmaceutical ingredient (API) without using a polymer.^{7,8} Therefore, the use of an appropriate cocrystal has the potential to address abovementioned problems when developing an extended release tablet using the conventional formulation approaches.

Cocrystals are crystalline materials consisting of two or more different molecules within the same crystal lattice in a definite stoichiometric ratio by non-covalent bonds, including but not limited to hydrogen bonds, π - π interactions, and Van der Waals forces.⁹ They manifest broad applicability and high flexibility through the judicious selection of a wide range of cofomers, providing opportunities to develop combination therapies, such as drug-drug,¹⁰⁻¹² drug-herb,¹³ herb-herb¹⁴ cocrystals for various diseases, where drug-drug cocrystal is advocated as fixed-dose combination product by the US Food and Drug Administration (FDA).⁹ In addition, the recognition of cocrystals as drug product intermediates rather than new chemical entities by the FDA^{9,15} has remarkably accelerated the translation of cocrystal research to clinical applications. Thus far, the FDA has approved several cocrystal products, such as Lexapro[®] and Entresto[®] for treating depression and heart failure, respectively.

Since the solubilities of parent molecules and cocrystals are inter-related,¹⁶ it is a possibility to obtain extended-release of a soluble drug by cocrystallization with a hydrophobic cofomer. Extensive studies have demonstrated that cocrystallization can significantly enhance physicochemical properties, such as solubility, dissolution rate, hygroscopicity, and stability of drugs,^{8,17,18} only limited research has probed into the use of cocrystals for achieving extended release of highly water-soluble drugs and most of cases could only achieve extended drug release

profiles lasting for no more than 6 h. Hence, it is of interest to prepare cocrystals capable of maintaining drug release over a longer period of time.

Tuberculosis (TB) is a common infectious disease caused by *Mycobacterium tuberculosis*, leading to around 1.3 million deaths among HIV-negative people accompanied with 300,000 deaths of HIV-positive patients worldwide in 2017.¹⁹ The current TB treatment regimen is daily or intermittent oral co-administration of four first-line drugs, namely isoniazid (INH), rifampicin (RIF), pyrazinamide, and ethambutol, for two months followed by INH and RIF combination treatment for four months and consolidation for one to two years.²⁰ This prolonged treatment leads to poor patient compliance, costs for directly observed therapy (DOT), hepatotoxicity, and the occurrence of multidrug-resistant tuberculosis (MDR-TB),²⁰ which substantially affects the efficacy of the drugs. Therefore, the development of extended release delivery systems is in demand to improve current TB therapy. Various carrier systems have been studied for this purpose, including nanoparticles and polymer-based systems.^{21, 22} However, the presence of polymers and other excipients in these delivery systems may alter the physiochemical properties and pharmacokinetics, thus leading to the issues of variable bioavailability and stability. Furthermore, conventional extended release technologies using polymer do not allow the breakage of tablets as their integrity ensures the extended release function, while extended-release cocrystal tablets could be splitted into appropriate proportions for patients' administration as doctors' advice, improving the dosing flexibility in clinical practice.

To this end, the goal of this study was to prepare an extended release INH cocrystal with curcumin (CUR). The pyridine ring, carbonyl group, and three hydrogen bond donors of INH are known functional groups capable of forming supramolecular structures.²³ Consequently, INH could cocrystallize with diverse cofomers, such as dicarboxylic acids, 4-aminosalicylic acid and gallic acid.^{10, 24, 25} The INH based TB treatment regimen is faced with two problems, 1) INH tablet is prone to oxidative degradation under high temperature and humidity conditions (40 °C, 75% RH),²⁶ 2) the presence of INH leads to erratic bioavailability of RIF in the acidic gastric environment.²⁷ We hypothesized that cocrystallization of INH with CUR, a poorly water-soluble polyphenolic compound extracted from the plant *Curcuma longa*, can address both stability problems. RIF was included in the following degradation and dissolution studies to mimic the clinical situation. A cocrystal with CUR was expected because CUR possesses two hydrogen bond donors and six hydrogen bond acceptors, illustrating a high probability for cocrystal formation, as

shown by several known CUR cocrystals with both phenols (e.g., resorcinol, pyrogallol and phloroglucinol)^{17, 28, 29} and non-phenols (e.g., 4, 4'-bipyridine-N,N'dioxide, nicotinamide and piperazine).³⁰ Such a cocrystal between the poorly water-soluble CUR (7.8 µg/mL)³¹ and highly water-soluble INH is expected to retard the solubility and dissolution rate of INH while also enhancing the dissolution performance and bioavailability of CUR to take advantage of its antitumor,³² anti-inflammatory,¹³ anti-HIV,³³ and anti-oxidative properties.³⁴ Recent study also suggested CUR acts as an inducer of caspase-3-dependent apoptosis and autophagy and protects against *Mycobacterium tuberculosis* infection in human macrophages, via the inhibition of nuclear factor-kappa B (NFκB) activation.³⁵ The high safe dose of curcumin, up to 12 g/day, in humans,³¹ also suggests good safety profiles of such a INH-CUR cocrystal.

2. Experimental Section

2.1. Materials

Isoniazid (INH, purity ≥ 99%) was supplied by Sigma-Aldrich (St. Louis, MO, USA). Curcumin (CUR, purity >99.5%) was purchased from Yung Zip Chemical (Taiwan, China). Rifampicin (RIF, purity >99.5%) was obtained from Yick-vic Chemicals & Pharmaceuticals (HK) Ltd (Hong Kong, China). Ethanol (EtOH) of analytical grade was sourced from Merck KGaA (Darmstadt, Germany). Water used was collected by a Direct-Q water purification system (Water Corp., Milford, MA, USA). All chemicals and solvents were used as received.

2.2. Preparation of Cocrystals

128 mg (0.933 mmol) INH and 172 mg (0.467 mmol) CUR in a 2:1 stoichiometric ratio were dissolved in 100 mL of EtOH under mild sonication. The solution was subjected to either slow evaporation or rapid solvent removal. For slow evaporation, the solution was placed in a fume hood until complete dryness. For rapid solvent removal, solvent was removed by a rotary evaporator (Buchi, Germany) equipped with a rotary flask immersed in a 60 °C water bath with different rotating speeds (10, 40, 80, 100 and 132 rpm) under vacuum. The resulting product was further dried in an oven at 60 °C overnight. All samples were gently triturated with mortar and pestle, and stored in sealed plastic vials with tinfoil to minimize any possible photo-degradation and moisture sorption.

2.3 Differential Scanning Calorimetry (DSC)

Thermograms were generated and recorded on a DSC 250 differential scanning calorimeter (TA Systems, USA). Indium standard was used for calibration prior to sample analysis. Samples were accurately weighed (1–3 mg) and loaded in hermetically sealed aluminum pans, held at 50 °C for 5 min and then heated from 50 °C to 250 °C at a scanning rate of 10 °C/min under nitrogen purge. Same experimental conditions were applied to collect data for constructing a temperature-composition phase diagram. Thermal data were collected and analyzed using the built-in TA TRIOS analysis software.

2.4. Powder X-Ray Diffraction (PXRD)

A MiniFlex 600 Diffractometer (Rigaku, Tokyo, Japan) equipped with Cu-K α radiation ($\lambda = 1.54056 \text{ \AA}$, 40 kV, 15 mA) and scintillation counter detector was utilized to collect the X-ray powder diffraction data. Sample was packed in an aluminum holder and scanned over a 2θ interval of $3^\circ - 45^\circ$ at 0.02° step size with a 4° per minute scanning rate.

2.5. Fourier-Transform Infrared (FTIR) Spectroscopy

FTIR spectrum was collected with an FTIR spectrophotometer (ALPHA, Bruker, Germany) in potassium bromide (KBr) diffuse reflectance mode. Sample was mixed with KBr in a ~1:20 w/w ratio and compressed into a thin disc by using a hydraulic press under two tons of force. The scan range was $4,000 \text{ cm}^{-1}$ to 500 cm^{-1} at a resolution of 4 cm^{-1} . A total of 16 scans were collected and average to arrive at a spectrum for each sample.

2.6. High Performance Liquid Chromatography (HPLC)

The concentrations of RIF, INH and CUR in the dissolution study were determined using an HPLC system coupled with a diode array detector (1200 series, Agilent Technologies, USA) and an Agilent Zorbax Eclipse Plus C18 column ($5 \mu\text{m}$, $250 \text{ mm} \times 4.6 \text{ mm}$). The mobile phase consisted of a gradient of acetonitrile (A) and 0.1M KH_2PO_4 buffer solution adjusted to pH 6.9 with NaOH (B). The gradient flow setting is as following: (1) 0-2 min, A: 50%, B: 50%; (2) 2-6 min, A: 40%, B: 60%; (3) 6-8 min, A: 50%, B: 50%. Absorbance was measured at 254 nm for RIF and INH and 425 nm for CUR. This method was validated for linearity ($R^2 = 0.9996$ for RIF, 0.9999 for INH, and 1.000 for CUR) by dissolving RIF and INH in a pH 1.2 buffer solution used

in the dissolution study, and CUR was dissolved in the mixture of 1:1 pH 1.2 buffer solution and acetonitrile due to its insolubility in aqueous solution. These stock solutions were prepared within the concentration range of 12-200 µg/mL, 6-100 µg/mL, and 9-150 µg/mL for RIF, INH, and CUR, respectively. As RIF would degrade rapidly in acidic condition, RIF solutions were injected for HPLC analysis immediately after being prepared. Sample solutions were injected after filtering through 0.45 µm membrane with fixed injection volume (20 µL) and flow rate (1 mL/min).

2.7. Dissolution Study

The dissolution study was performed by using a Copley Dissolution Tester DIS8000 (Copley Scientific Limited, UK). RIF, INH, CUR and INH-CUR cocrystal powders were sifted within the range of 125-180 µm using standard sieves (VWR International, New York, USA) to minimize the variations in particle size and morphology. About 150 mg RIF, 75 mg INH, 101 mg CUR and 176 mg INH-CUR cocrystal powders were encapsulated into size 0 gelatin capsules (Capsugel, Suzhou, China). They were divided into four groups, including RIF, RIF+INH, RIF+INH+CUR and RIF+INH-CUR cocrystal. These capsules enclosed within sinkers were placed into 900 mL pH 1.2 and pH 6.8 buffers separately to obtain their dissolution profiles at 37 °C. Paddle method was used and the rotating speed was set at 100 rpm. At the designated time points, i.e., 15 min, 30 min, 45 min, 60 min, 90 min, 2 h, 4 h, 6 h, 8 h, 10 h, 18 h, 24 h and 48 h, 3 mL solution was withdrawn by a syringe and same volume of buffer solution was added back into the vessel. The collected solution was filtered by a 0.45 µm nylon filter followed by HPLC assay. The remaining powders after dissolution tests were collected for PXRD and DSC analysis. All results were conducted in triplicate.

As RIF follows first-order degradation kinetics,³⁶ its degradation rate constant could be obtained by fitting the data in Eq. 1:

$$\ln(C_f) = \ln(C_0) - K_d t \quad (\text{Eq. 1})$$

where C_f is the concentration of RIF at time t , C_0 is the initial concentration, K_d represents degradation constant (min^{-1}) and t is time shown in minutes.

In order to explore the release mechanism of INH from the cocrystal, the release data were separately fitted into the following mathematical models.³⁷

Zero order kinetics: $Q_t = K_0 t$ (Eq. 2)

First order kinetics: $\log Q_t = \log Q_0 + \frac{K_1 t}{2.303}$ (Eq. 3)

Higuchi's equation: $Q_t = K_H t^{1/2}$ (Eq. 4)

Korsmeyer-Peppas equation: $Q_t = K_{kp} t^n$ (Eq. 5)

where, Q_0 is the initial percent of INH in solution, Q_t is the percent of INH released at time t ; K_0 , K_1 , K_H and K_{kp} are the rate constants of zero order, first order, Higuchi's and Korsmeyer-Peppas models, respectively. The value n in Korsmeyer-Peppas equation is the release exponent and can be used to characterize INH transport mechanism.

2.8. Dynamic Vapor Sorption (DVS)

A moisture balance (Intrinsic DVS, Surface Measurement Systems Ltd., Allentown, PA, USA) was used to obtain water sorption-desorption isotherm at 25 °C with nitrogen flow rate at 50 mL/min. A sample was placed in a quartz sample and equilibrated at each step for meeting the equilibration criteria of either $dm/dt < 0.003\%$ or maximum equilibration time of 6 h. If one of the criteria was met, the relative humidity (RH) would change to next target value within a 0% – 95% – 0% RH cycle with a step size of 5%.

2.9. Statistical analysis

Statistical analysis was performed by one-way ANOVA using PRISM 7 software (Graphpad Software Inc., San Diego, CA, USA). Differences were considered as statistically significant if $p < 0.05$.

3. Results and Discussion

3.1. Cocrystallization of Isoniazid with Curcumin

The phase purity of the INH-CUR samples prepared by slow and rapid solvent evaporation was analyzed by PXRD (Fig. 2) based on the characteristic peaks at 2θ diffraction angles of the corresponding cocrystal formers (i.e., INH: 11.95° and 19.64°, and CUR: 7.87° and 8.85°). For

sample obtained by slow evaporation, the PXRD pattern was a superposition of the cocrystal formers, implying the product was simply a physical mixture of INH and CUR. As for the sample prepared by rapid solvent removal, the characteristic peaks corresponding to INH and CUR were absent and two distinct diffraction peaks (i.e., $2\theta = 13.08^\circ$ and 20.24°) were seen in the PXRD pattern. This indicates the effectiveness of rapid solvent removal in preparing INH-CUR cocrystal through kinetic entrapment, as observed in other systems.^{17, 38} Moreover, INH-CUR cocrystal exhibited a bright orange color, which was different from the white color of INH and bright yellow color of CUR (Fig. S1).

3.2. Thermal Properties and Stability

The DSC thermograms of INH, CUR, and INH-CUR cocrystal (Fig. 3) suggest that the 2:1 INH-CUR cocrystal exhibited a sharp melting endotherm at 156°C , which was lower than those of INH (175°C) and CUR (183°C). The fusion enthalpy of INH-CUR cocrystal ($\Delta H_f = 90.17$ kJ/mol) was significantly higher than those of both INH ($\Delta H_f = 33.17$ kJ/mol) and CUR ($\Delta H_f = 49.02$ kJ/mol), suggesting a stronger crystal lattice was formed upon cocrystallization. For further examination of the new cocrystal and confirmation of its stoichiometry ratio, a temperature-composition phase diagram of INH-CUR system was constructed from DSC data of INH and CUR binary mixtures (Fig. 4). The phase diagram embraced two eutectic points and displayed a typical W-shaped pattern for a binary cocrystal system.³⁹ The congruent melting point at 0.67 INH molar composition confirmed a 2:1 stoichiometry of the INH-CUR cocrystal. Two eutectic points were located at 0.57 and 0.78 INH mole fractions with eutectic melting at 142.1°C and 141.1°C , respectively. After confirmation of INH-CUR cocrystal, pure INH, CUR, and INH-CUR cocrystal samples were separately sealed in glass vials and stored at 60°C in a dry environment ($\text{RH} = 3\%$) for 1 month to examine their thermal stability. The PXRD patterns and thermograms for all samples remain essentially unchanged (Fig. S2), suggesting they were physically stable under these conditions. The key thermal properties of the INH, CUR, and INH-CUR cocrystal are summarized in Table 1.

3.3. Effect of solvent evaporation rate on phase purity

Phase purity of metastable cocrystals prepared by kinetic entrapment is expected to depend on the rate of solvent removal. To examine this effect on the phase purity of INH-CUR cocrystal,

samples were prepared at different rotary speeds (10, 40, 80, 100 and 132 rpm) of the rotary evaporator and analyzed using DSC. Interestingly, when the rotary speed was ≤ 40 rpm, peaks corresponding to eutectic melting were observed in the DSC profiles (Fig. 5), indicating incomplete cocrystal conversion. However, when the rotary speed was ≥ 80 rpm, one sharp endotherm at 156 °C, corresponding to that of the INH-CUR cocrystal, was produced. Clearly, evaporation rate was a critical processing parameter that governs the cocrystal nucleation and growth kinetics and the phase purity of the INH-CUR cocrystal. Considering the different designs and configurations of different rotary evaporators, solvent removal rates corresponding to the rotary speeds were determined. The rotary speeds 10 rpm and 80 rpm correspond to solvent evaporation rates of 6 and 8.4 mL/min, respectively. Both 100 and 132 rpm rotary speeds corresponded to the essentially same evaporation rate as that of 80 rpm.

3.4. FTIR Spectroscopic Analysis

The stretching vibration of phenolic O-H of CUR located at 3506 cm^{-1} dramatically shifted to a lower wavenumber at 3423 cm^{-1} in the INH-CUR cocrystal along with the change in peak shape from sharp to broad (Fig. 6), suggesting the formation of strong intermolecular hydrogen bonds.⁴⁰ In addition, the primary amine N-H stretching frequency of INH changed from 3305 cm^{-1} to 3311 cm^{-1} in INH-CUR cocrystal as well as pyridine ring C-N stretching frequency shifted from 1335 cm^{-1} to 1275 cm^{-1} , indicating their chemical environment have been altered upon cocrystallization.^{10, 41} Interestingly, the amide N-H stretching frequency of INH at 3111 cm^{-1} was nearly absent in the FTIR spectra of INH-CUR cocrystal. The key features of the FTIR spectra of INH, CUR, and their cocrystal are provided in Table 2.

3.5. Dynamic Vapor Sorption and SEM analysis

The DVS isotherms of INH, CUR and INH-CUR cocrystal (Fig. S3) suggest that both INH and CUR were non-hygroscopic as their amounts of water sorption were less than 0.3% even at 95% RH. The INH-CUR cocrystal adsorbed $\sim 1\%$ moisture at 95% RH. The slightly higher moisture sorption by the INH-CUR cocrystal is at least partially attributed to its rough surfaces, hence larger surface area than those of coformer powders (Fig. S4). The presence of a small amount of surface moisture (1-5%) in drugs and excipients (e.g., microcrystalline cellulose) is not uncommon, which can sometimes benefit tableting.⁴²

3.6. Dissolution Measurement

3.6.1. Degradation of RIF

The presence of INH would accelerate the degradation of RIF in the acidic solution.²⁷ Given that INH and RIF are used for combination therapy at least for 6 months in current clinical practice, any impact of cocrystallization on stability of RIF is likely clinically significant.⁴³ Therefore, the effects of cocrystallization on dissolution profile and degradation kinetics of RIF in pH 1.2 buffer solution were evaluated by comparing properties of four powders, i.e., RIF, RIF+INH, RIF+INH+CUR, and RIF+INH-CUR. Sieved RIF, INH, CUR and INH-CUR cocrystal powders with 125-180 μm size were used in order to minimize the effects of particle size. Consistent with the literature report, RIF underwent rapid degradation in pH 1.2 buffer solution, with about 40% degraded at 90 minutes in all groups (Fig. 7A). To quantitatively analyze the degradation kinetics, RIF concentrations at 15 minutes (C_{15}) and 90 minutes were regarded as the initial concentration C_0 and C_f in the Eq. 1, respectively. The apparent degradation rate constant (K_d) of RIF, obtained by fitting the results into the first order degradation kinetic model, was $0.67 \times 10^{-3} (\pm 1.33 \times 10^{-4}) \text{ min}^{-1}$. The degradation rate of RIF in the RIF+INH group was the highest, with $K_d = 0.89 \times 10^{-3} (\pm 4.66 \times 10^{-5}) \text{ min}^{-1}$. The K_d of the RIF+INH-CUR sample ($0.77 \times 10^{-3} \pm 6.60 \times 10^{-5} \text{ min}^{-1}$) was slightly lower than those of RIF+INH and RIF+INH+CUR ($0.84 \times 10^{-3} \pm 4.47 \times 10^{-5} \text{ min}^{-1}$) groups. However, the differences were not statistically significant among all four groups ($p > 0.05$).

3.6.2 Dissolution profiles at pH 1.2 and 6.8

At pH 1.2, INH in both RIF+INH and RIF+INH+CUR groups was completely released within 15 min. In contrast, only 28% of INH was released from the INH-CUR cocrystal at 15 min (Fig. 7B), followed by slow extended release of $\sim 73\%$ of INH over a period of 48 h. The slower release of INH from the cocrystal could be explained by the reduced cocrystal solubility, partly due to the blockage of INH solvation sites by CUR.⁴⁴

According to Good and Rodriguez-Hornedo,¹⁶ the solubility of a cocrystal of a drug positively correlates with the solubility of coformers. Given the extremely low solubility of CUR, the dissolution of INH from the cocrystal is expected to be retarded due to the reduced solubility of INH-CUR. The cocrystal solubility is also influenced by the stoichiometric ratio of cocrystal

(Eq. 6).¹⁶ As the INH-CUR cocrystal is in a 2:1 molar ratio, highly water soluble INH apparently dominates the cocrystal solubility and facilitates initial cocrystal dissolution. When the cocrystal started to contact with the dissolution medium, the surface INH-CUR cocrystal dissolved rapidly in a molecular cocrystal form and thus led to an initial burst release of INH. (Eq. 6),

$$S_{A_{\alpha}B_{\beta}} = \sqrt[\alpha+\beta]{K_{sp}/\alpha^{\alpha}\beta^{\beta}} \quad (\text{Eq. 6})$$

where A is drug, B is cocrystal former, K_{sp} is the solubility product of the cocrystal, α and β are the stoichiometric ratios of A and B, respectively.

During the dissolution studies, there was an interesting phenomenon that the pH 1.2 dissolution medium started to become turbid after 4 h (Fig. S5A), which indicates precipitation likely occurred. The release profile of CUR was similar to INH in INH-CUR cocrystal for the first 4 h as concentration of CUR continued to rise (Fig. 8A). However, the concentration of CUR declined after 4 h, and became undetectable after 12 h. Based on the HPLC results and literature data,⁴⁵ the drop in CUR assay was mainly due to recrystallization of CUR from the solution but not chemical degradation. The release of CUR from the raw CUR powder and physical mixture of RIF+INH+CUR was non-detectable throughout the dissolution study. Thus, the INH-CUR cocrystal significantly improved the release of CUR. It is worth to note that the recrystallized CUR was form III polymorph instead of the thermodynamically most stable form I used in the present study (Fig. S6).⁴⁶ However, it has been reported that CUR form I precipitated out when curcumin-resorcinol and curcumin-pyrogallol cocrystals were dispersed in 40 % EtOH-water after 4 h.²⁸ Two possible mechanisms may explain the observation of different CUR polymorphs in these examples. The first possibility is that the presence of coformer INH facilitated the nucleation of CUR form III during precipitation, which remained kinetically stable in the aqueous medium in this study due to the very low solubility. However, the slow evaporation of INH and CUR did not result in a form III curcumin based on PXRD pattern (Fig. 2). Hence, this mechanism is not prevailing in the process of CUR form III precipitation in this work. The second mechanism is the difference in the degree of CUR supersaturation. As curcumin could dissolve much more in 40% EtOH-water than pH 1.2 buffer, the dissolution of INH-CUR cocrystal resulted in a much higher degree of supersaturation of CUR than those by curcumin-resorcinol and curcumin-pyrogallol cocrystals. According to Ostwald's rule of stage, the less stable form III tended to crystallize out first under a

higher degree of supersaturation.⁴⁷ The metastable form III remained kinetically stable in pH 1.2 medium due to the very slow mass transfer limited by the very low solubility. The precipitation of poorly soluble CUR likely had coated the undissolved INH-CUR cocrystal particle surfaces, as observed before in other CUR cocrystals.¹⁷ Moreover, CUR is more stable at low pH,⁴⁸ so the *in situ* coating by CUR, in turn, provides an extended release mechanism of INH.

To further investigate the release mechanism of INH from the cocrystal, dissolution of the cocrystal was also studied at pH 6.8 (Fig. 9). Unlike the situation at pH 1.2, a complete release of INH was obtained from the cocrystal after 48 h at pH 6.8. The difference between the release profiles of INH in the two media could be ascribed to the distinct recrystallization kinetic of CUR and the degradation of INH at low pH with the presence of RIF (about 6% INH degraded at 90 min based on the HPLC result). In the pH 6.8 study, the less CUR release could be partially due to the instability of CUR at neutral and basic conditions.⁴⁵ The schematic present in Fig. 10 illustrates the proposed mechanism of INH-CUR cocrystal dissolution at pH 1.2 and pH 6.8. For the first 4 h, the INH release profiles for both buffers were similar, and INH released slightly faster at pH 1.2 because the solubility behavior of the cocrystal acted like basic INH rather than acidic CUR. Recrystallization of CUR form III was seen after 4 h in the pH 6.8 medium as well (Fig. 8B). However, the amount of the recrystallized CUR was much lower at pH 6.8 than that at pH 1.2. In addition to the amount of precipitating CUR, the CUR form III recrystallized from the pH 1.2 medium exhibited a relatively lower crystallinity (Fig. S6) and smaller size (Fig. S7). The smaller particles tended to suspend in the dissolution medium to cause higher turbidity. The release of INH from the cocrystal were also fitted into four common kinetics models, including zero order, first order, Korsmeyer-Peppas and Higuchi models (Table 3). The fitting by the Korsmeyer-Peppas model was the best at both pHs (with $R^2 > 0.98$). The lower than 0.45 n values in both pH media indicated the INH release followed the mechanism of Fickian diffusion.⁴⁹

The dissolution results demonstrated that cocrystallization is a promising formulation strategy for achieving extended release of water-soluble drugs without using polymers. As recommended by WHO, Directly Observed Therapy by nurses or family members is required for anti-TB treatment. Reformulating INH using the extended release cocrystal has clinical advantage by reducing dosing frequency, increasing dosing flexibility and improving patient compliance.

4. Conclusion

We have prepared and characterized a new 2:1 INH-CUR cocrystal using rapid solvent removal. The solvent evaporation rate was a critical processing parameter for controlling the phase purity of the resulting cocrystal. Importantly, we have demonstrated the effectiveness of cocrystallization for attaining extended release of highly water soluble INH. To the best of our knowledge, this is the first study reporting the use of cocrystal to achieve sustained drug release up to 48 h. Our finding exemplifies the potential use of cocrystals for extended drug release, which is clinically important for a number of diseases requiring the maintenance of an optimal drug concentration in blood over a long time period.

Acknowledgements

The work was financially supported by the Li Ka Shing Faculty of Medicine (Project number: 204600519) and University Research Committee (Project number: 104004777) at The University of Hong Kong. We also thank Mr. Ray H. W. Lee at the University of Hong Kong for his assistance with the dissolution study.

Supporting Information

PXRD patterns, stability profiles, DVS isotherm, SEM images, dissolution behaviour and related DSC, PXRD and SEM data

References

1. Natarajan, J. V.; Nugraha, C.; Ng, X. W.; Venkatraman, S. Sustained-release from nanocarriers: a review. *J. Control. Release* **2014**, *193*, 122-138.
2. Ummadi, S. S., B.; Rao, N. G. R.; Reddy, M. S.; Sanjeev, B. Overview on controlled release dosage form. *Int. J. Pharma Sci.* **2013**, *3*, 258-269.
3. Tiwari, S. B.; Rajabi-Siahboomi, A. R. Extended-Release Oral Drug Delivery Technologies: Monolithic Matrix Systems. In *Drug Delivery Systems*, Jain, K. K., Ed. Humana Press: Totowa, NJ, 2008; pp 217-243.
4. Hwang, S.; Maitani, Y.; Qi, X.-R.; Takayama, K.; Nagai, T. Remote loading of diclofenac, insulin and fluorescein isothiocyanate labeled insulin into liposomes by pH and acetate gradient methods. *Int. J. Pharm.* **1999**, *179*, 85-95.
5. Chang, H.-I.; Yeh, M.-K. Clinical development of liposome-based drugs: formulation, characterization, and therapeutic efficacy. *Int J Nanomedicine* **2012**, *7*, 49-60.
6. Noyes, A. A.; Whitney, W. R. The rate of solution of solid substances in their own solutions. *J. Am. Chem. Soc* **1897**, *19*, 930-934.
7. Sun, C. C. Cocrystallization for successful drug delivery. *Expert Opin Drug Deliv* **2013**, *10*, 201-13.
8. Chow, S. F.; Chen, M.; Shi, L.; Chow, A. H.; Sun, C. C. Simultaneously improving the mechanical properties, dissolution performance, and hygroscopicity of ibuprofen and flurbiprofen by cocrystallization with nicotinamide. *Pharm. Res.* **2012**, *29*, 1854-65.
9. U.S. Food and Drug Administration, Regulatory Classification of Pharmaceutical Co-Crystals Guidance for Industry. Revision 1 ed.; Washington, DC, 2016.
10. Grobelny, P.; Mukherjee, A.; Desiraju, G. Drug-drug co-crystals: Temperature-dependent proton mobility in the molecular complex of isoniazid with 4-aminosalicylic acid. *CrystEngComm* **2011**, *13*, 4358.
11. Jiang, L.; Huang, Y.; Zhang, Q.; He, H.; Xu, Y.; Mei, X. Preparation and Solid-State Characterization of Dapsone Drug-Drug Co-Crystals. *Cryst. Growth Des.* **2014**, *14*, 4562-4573.
12. Karimi-Jafari, M.; Padrela, L.; Walker, G. M.; Croker, D. M. Creating Cocrystals: A Review of Pharmaceutical Cocrystal Preparation Routes and Applications. *Cryst. Growth Des.* **2018**, *18*, 6370-6387.
13. Chan, M. M.-Y.; Huang, H.-I.; Fenton, M. R.; Fong, D. In Vivo Inhibition of Nitric Oxide Synthase Gene Expression by Curcumin, a Cancer Preventive Natural Product with Anti-Inflammatory Properties. *Biochem. Pharmacol.* **1998**, *55*, 1955-1962.
14. Deng, Y.; Zhang, Y.; Huang, Y.; Zhang, M.; Lou, B. Preparation, Crystal Structures, and Oral Bioavailability of Two Cocrystals of Emodin with Berberine Chloride. *Cryst. Growth Des.* **2018**, *18*, 7481-7488.
15. Aitipamula, S.; Banerjee, R.; Bansal, A. K.; Biradha, K.; Cheney, M. L.; Choudhury, A. R.; Desiraju, G. R.; Dikundwar, A. G.; Dubey, R.; Duggirala, N.; Ghogale, P. P.; Ghosh, S.; Goswami, P. K.; Goud, N. R.; Jetti, R. R. K. R.; Karpinski, P.; Kaushik, P.; Kumar, D.; Kumar, V.; Moulton, B.; Mukherjee, A.; Mukherjee, G.; Myerson, A. S.; Puri, V.; Ramanan, A.; Rajamannar, T.; Reddy, C. M.; Rodriguez-Hornedo, N.; Rogers, R. D.; Row, T. N. G.; Sanphui, P.; Shan, N.; Shete, G.; Singh, A.; Sun, C. C.; Swift, J. A.; Thaimattam, R.; Thakur, T. S.; Kumar Thaper, R.; Thomas, S. P.; Tothadi, S.; Vangala, V. R.; Variankaval, N.; Vishweshwar, P.; Weyna, D. R.; Zaworotko, M. J. Polymorphs, Salts, and Cocrystals: What's in a Name? *Cryst. Growth Des.* **2012**, *12*, 2147-2152.

16. Good, D. J.; Rodríguez-Hornedo, N. Solubility Advantage of Pharmaceutical Cocrystals. *Cryst. Growth Des.* **2009**, *9*, 2252-2264.
17. Chow, S. F.; Shi, L.; Ng, W. W.; Leung, K. H. Y.; Nagapudi, K.; Sun, C. C.; Chow, A. H. L. Kinetic Entrapment of a Hidden Curcumin Cocrystal with Phloroglucinol. *Cryst. Growth Des.* **2014**, *14*, 5079-5089.
18. Smith, A. J.; Kavuru, P.; Wojtas, L.; Zaworotko, M. J.; Shytle, R. D. Cocrystals of Quercetin with Improved Solubility and Oral Bioavailability. *Mol. Pharm.* **2011**, *8*, 1867-1876.
19. World Health Organization, Global tuberculosis report 2018. 2018.
20. Pham, D. D.; Fattal, E.; Tsapis, N. Pulmonary drug delivery systems for tuberculosis treatment. *Int. J. Pharm.* **2015**, *478*, 517-29.
21. Dutt, M.; Khuller, G. K. Sustained release of isoniazid from a single injectable dose of poly (dl-lactide-co-glycolide) microparticles as a therapeutic approach towards tuberculosis. *Int. J. Antimicrob.* **2001**, *17*, 115-122.
22. Gangadharam, P. R. J.; Ashtekar, D. R.; Farhi, D. C.; Wise, D. L. Sustained release of isoniazid in vivo from a single implant of a biodegradable polymer. *Tubercle* **1991**, *72*, 115-122.
23. Sodanapalli, R.; Nair, R.; Bachala, T. Preparation and Pharmaceutical Characterization of Supra molecular Complex of Isoniazid with L(+) Tartaric acid. *J. Biomed. Sci. and Res.* **2011**, *3*, 397-402.
24. Sarcevic, I.; Orola, L.; Veidis, M. V.; Podjava, A.; Belyakov, S. Crystal and Molecular Structure and Stability of Isoniazid Cocrystals with Selected Carboxylic Acids. *Cryst. Growth Des.* **2013**, *13*, 1082-1090.
25. Kaur, R.; Perumal, S. S. R. R.; Bhattacharyya, A. J.; Yashonath, S.; Guru Row, T. N. Structural Insights into Proton Conduction in Gallic Acid–Isoniazid Cocrystals. *Cryst. Growth Des.* **2014**, *14*, 423-426.
26. Battini, S.; Mannava, M. K. C.; Nangia, A. Improved Stability of Tuberculosis Drug Fixed-Dose Combination Using Isoniazid-Caffeic Acid and Vanillic Acid Cocrystal. *J. Pharm. Sci* **2018**, *107*, 1667-1679.
27. Singh, S.; Mariappan, T. T.; Sharda, N.; Kumar, S.; Chakraborti, A. K. The Reason for an Increase in Decomposition of Rifampicin in the Presence of Isoniazid under Acid Conditions. *Pharm Pharmacol Comm* **2000**, *6*, 405-410.
28. Sanphui, P.; Goud, N. R.; Khandavilli, U. B. R.; Nangia, A. Fast Dissolving Curcumin Cocrystals. *Cryst. Growth Des.* **2011**, *11*, 4135-4145.
29. Sathisaran, I.; Dalvi, S. V. Crystal Engineering of Curcumin with Salicylic Acid and Hydroxyquinol as Coformers. *Cryst. Growth Des.* **2017**, *17*, 3974-3988.
30. Su, H.; He, H.; Tian, Y.; Zhao, N.; Sun, F.; Zhang, X.; Jiang, Q.; Zhu, G. Syntheses and characterizations of two curcumin-based cocrystals. *Inorg. Chem.* **2015**, *55*, 92-95.
31. Anand, P.; Kunnumakkara, A. B.; Newman, R. A.; Aggarwal, B. B. Bioavailability of Curcumin: Problems and Promises. *Mol. Pharm.* **2007**, *4*, 807-818.
32. Kunnumakkara, A. B.; Guha, S.; Krishnan, S.; Diagaradjane, P.; Gelovani, J.; Aggarwal, B. B. Curcumin Potentiates Antitumor Activity of Gemcitabine in an Orthotopic Model of Pancreatic Cancer through Suppression of Proliferation, Angiogenesis, and Inhibition of Nuclear Factor- κ B–Regulated Gene Products. *Cancer Res.* **2007**, *67*, 3853.
33. Jordan, W. C.; Drew, C. R. Curcumin--a natural herb with anti-HIV activity. *J Natl Med Assoc* **1996**, *88*, 333-333.
34. Selvam, R.; Subramanian, L.; Gayathri, R.; Angayarkanni, N. The anti-oxidant activity of turmeric (*Curcuma longa*). *J. Ethnopharmacol.* **1995**, *47*, 59-67.

35. Bai, X.; Oberley-Deegan, R. E.; Bai, A.; Ovrutsky, A. R.; Kinney, W. H.; Weaver, M.; Zhang, G.; Honda, J. R.; Chan, E. D. Curcumin enhances human macrophage control of Mycobacterium tuberculosis infection. *Respirology* **2016**, *21*, 951-957.
36. Shishoo, C. J.; Shah, S. A.; Rathod, I. S.; Savale, S. S.; Kotecha, J. S.; Shah, P. B. Stability of rifampicin in dissolution medium in presence of isoniazid. *Int. J. Pharm.* **1999**, *190*, 109-123.
37. Costa, P.; Sousa Lobo, J. M. Modeling and comparison of dissolution profiles. *Eur. J. Pharm. Sci* **2001**, *13*, 123-133.
38. Weng, J.; Wong, S. N.; Xu, X.; Xuan, B.; Wang, C.; Chen, R.; Sun, C. C.; Lakerveld, R.; Kwok, P. C. L.; Chow, S. F. Cocrystal Engineering of Itraconazole with Suberic Acid via Rotary Evaporation and Spray Drying. *Cryst. Growth Des.* **2019**, *19*, 2736-2745.
39. Stoler, E.; Warner, C. J. Non-Covalent Derivatives: Cocrystals and Eutectics. *Molecules* **2015**, *20*, 14833-14848.
40. Wong, S. N.; Hu, S.; Ng, W. W.; Xu, X.; Lai, K. L.; Lee, W. Y. T.; Chow, A. H. L.; Sun, C. C.; Chow, S. F. Cocrystallization of Curcumin with Benzenediols and Benzenetriols via Rapid Solvent Removal. *Cryst. Growth Des.* **2018**, *18*, 5534-5546.
41. Aitipamula, S.; Wong, A. B. H.; Chow, P. S.; Tan, R. B. H. Novel solid forms of the anti-tuberculosis drug, Isoniazid: ternary and polymorphic cocrystals. *CrystEngComm* **2013**, *15*, 5877-5887.
42. Khan, F.; Pilpel, N. The effect of particle size and moisture on the tensile strength of microcrystalline cellulose powder. *Powder Technol.* **1986**, *48*, 145-150.
43. Lai, J. M. L.; Yang, S. L.; Avoi, R. Treating More with Less: Effectiveness and Event Outcomes of Antituberculosis Fixed-dose Combination Drug versus Separate-drug Formulation (Ethambutol, Isoniazid, Rifampicin and Pyrazinamide) for Pulmonary Tuberculosis Patients in Real-world Clinical Practice. *J Glob Infect Dis* **2019**, *11*, 2-6.
44. Aitipamula, S.; Cadden, J.; Chow, P. S. Cocrystals of zonisamide: physicochemical characterization and sustained release solid forms. *CrystEngComm* **2018**, *20*, 2923-2931.
45. Wang, Y.-J.; Pan, M.-H.; Cheng, A.-L.; Lin, L.-I.; Ho, Y.-S.; Hsieh, C.-Y.; Lin, J.-K. Stability of curcumin in buffer solutions and characterization of its degradation products. *J. Pharm. Biomed. Anal.* **1997**, *15*, 1867-1876.
46. Sanphui, P.; Goud, N. R.; Khandavilli, U. B. R.; Bhanoth, S.; Nangia, A. New polymorphs of curcumin. *ChemComm.* **2011**, *47*, 5013-5015.
47. Van Santen, R. A. The Ostwald step rule. *J. Phys. Chem.* **1984**, *88*, 5768-5769.
48. Kumavat, S.; Chaudhari, Y.; Borole, P.; Mishra, P.; Shenghani, K.; Duvvuri, P. Degradation studies of curcumin. *Int. J Pharm Rev Res* **2013**, *3*, 50-55.
49. Peppas, N. Analysis of Fickian and non-Fickian drug release from polymers. *Pharm Acta Helv* **1985**, *60*, 110-111.

Tables

Table 1. The thermal properties of the INH, CUR and INH cocrystal

Sample	Melting point (°C)	Eutectics melting (°C)	ΔH_f (kJ/mol)
INH	175	—	33.17
CUR	183	—	49.02
INH-CUR	156	142.1, 141.1	90.17

Table 2. The key features in the FTIR spectra of INH, CUR and INH-CUR cocrystal.

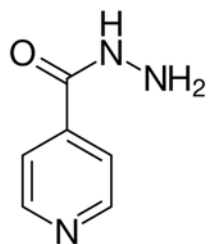
Sample	Phenolic O-H stretching / cm^{-1}	Amide N-H stretching / cm^{-1}	C=O stretching / cm^{-1}	Aromatic C=C / cm^{-1}	Pyridine ring C-N stretching / cm^{-1}
INH	—	3305, 3111	1667	—	1335
CUR	3506	—	1627	1603	—
INH-CUR	3423	3311	—	—	1275

Table 3. Dissolution kinetics of INH in pH 1.2 and pH 6.8 buffer.

Formula	Zero order		First order		Higuchi		Korsmeyer-Peppas		
	R^2	K_0 (min^{-1})	R^2	K_1 (min^{-1})	R^2	K_H ($\text{min}^{-1/2}$)	R^2	K_{KP} (min^{-n})	n
pH 1.2	0.7391	0.0383	0.3932	0.0025	0.8874	1.9249	0.9976	17.5577	0.1804
pH 6.8	0.8869	0.0505	0.5361	0.0026	0.9775	2.3447	0.9889	7.2078	0.3397

Figures

(A)



(B)

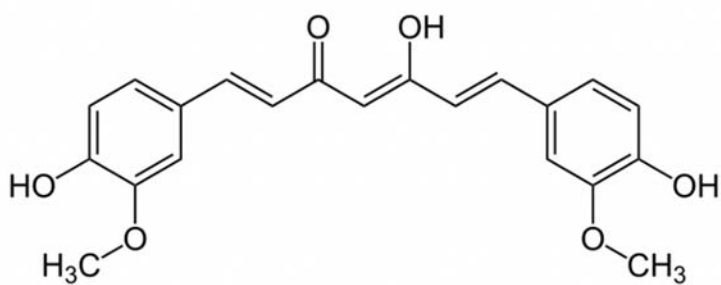


Figure 1. Chemical structures of (A) isoniazid (INH) and (B) curcumin (CUR).

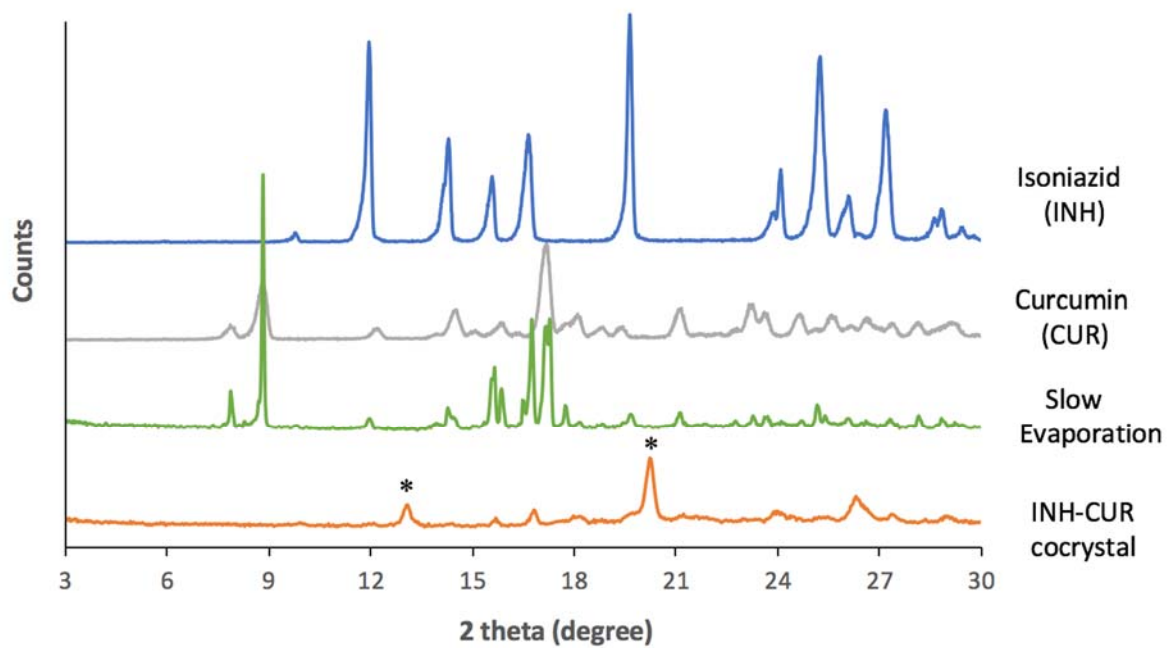


Figure 2. PXRD patterns of INH, CUR, INH-CUR product made by slow evaporation and 2:1 INH-CUR cocrystal. The characteristic peaks of INH-CUR cocrystal were marked with *.

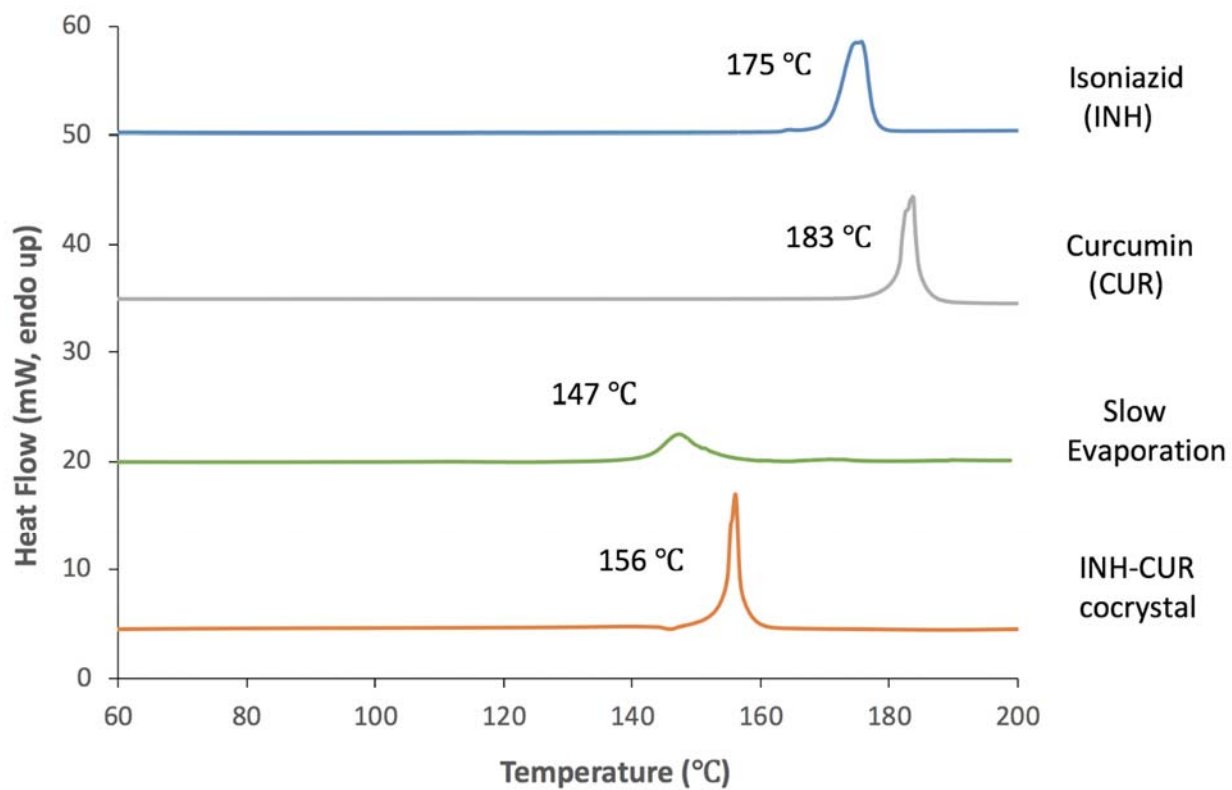


Figure 3. Overlaid DSC profiles of INH, CUR, INH-CUR product prepared by slow evaporation and 2:1 INH-CUR cocrystal prepared by rapid solvent removal.

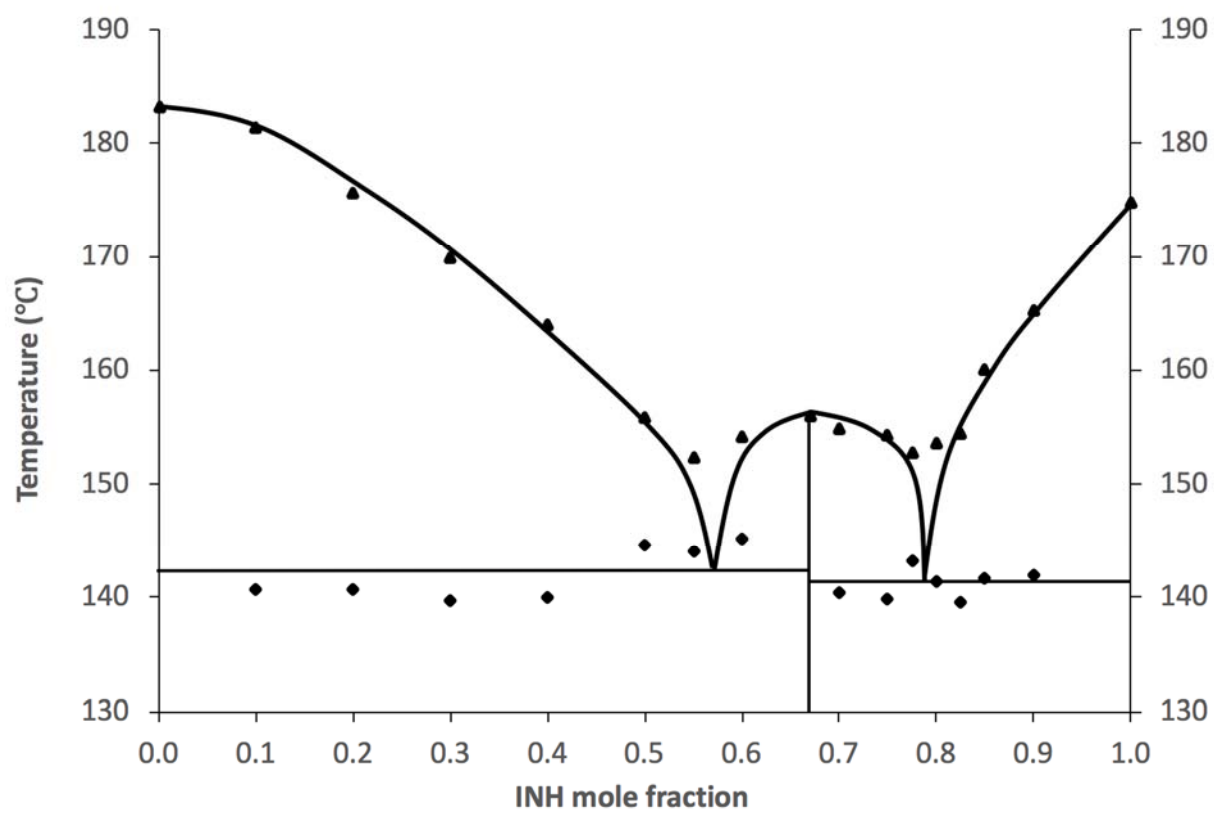


Figure 4. Temperature – composition phase diagram of the INH-CUR cocrystal system.

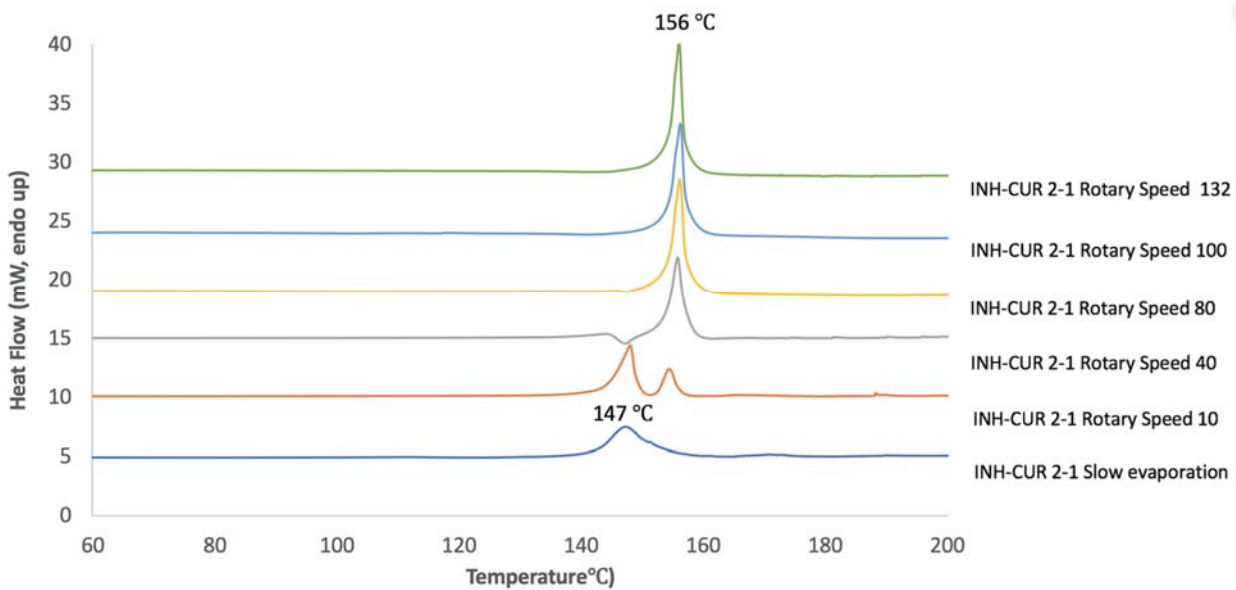


Figure 5. Effect of solvent evaporation rate on phase purity of INH-CUR cocrystal by DSC analysis.

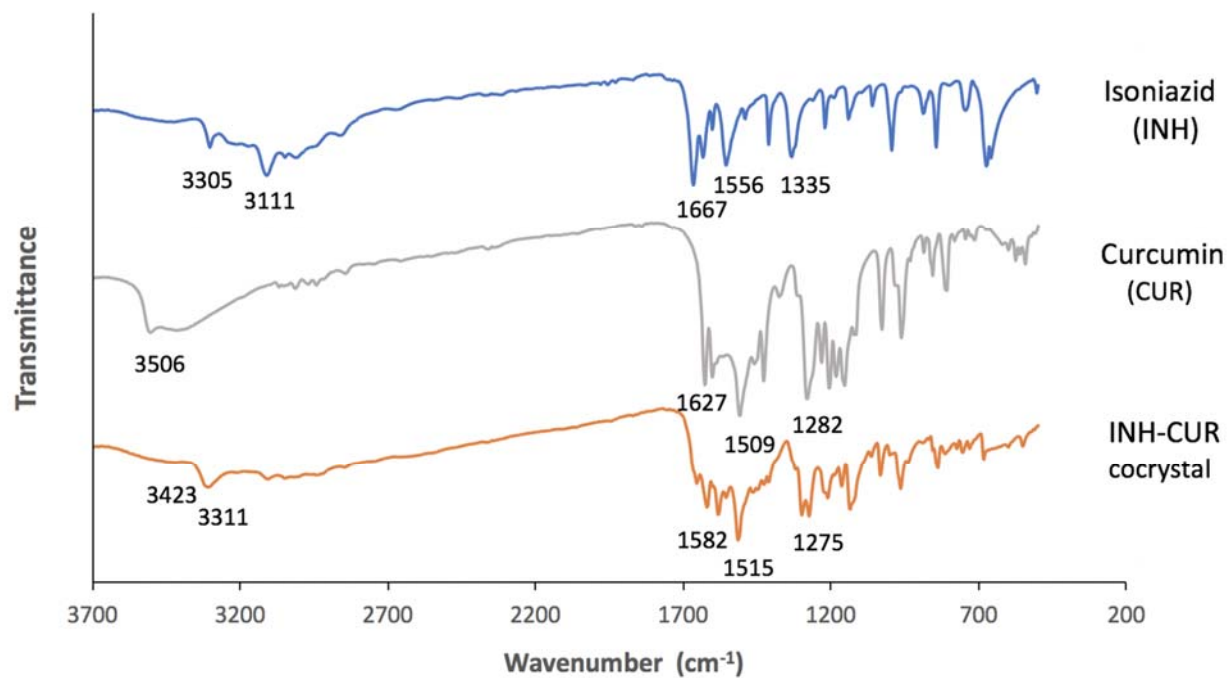
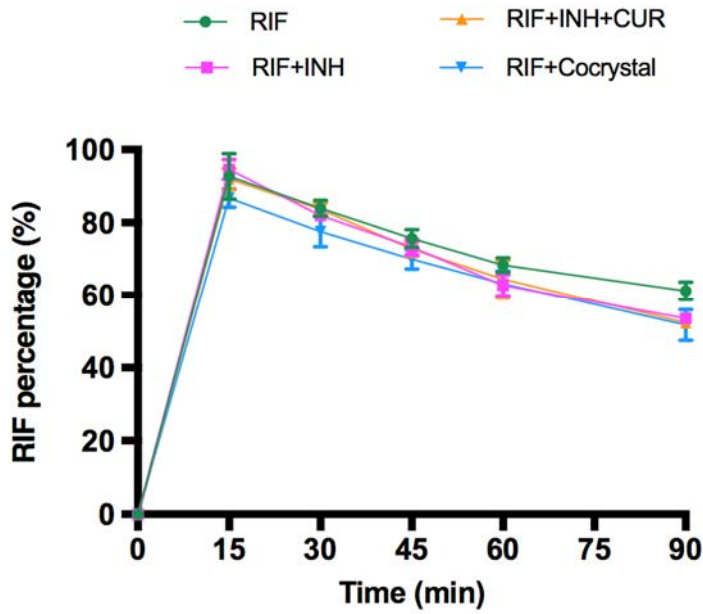


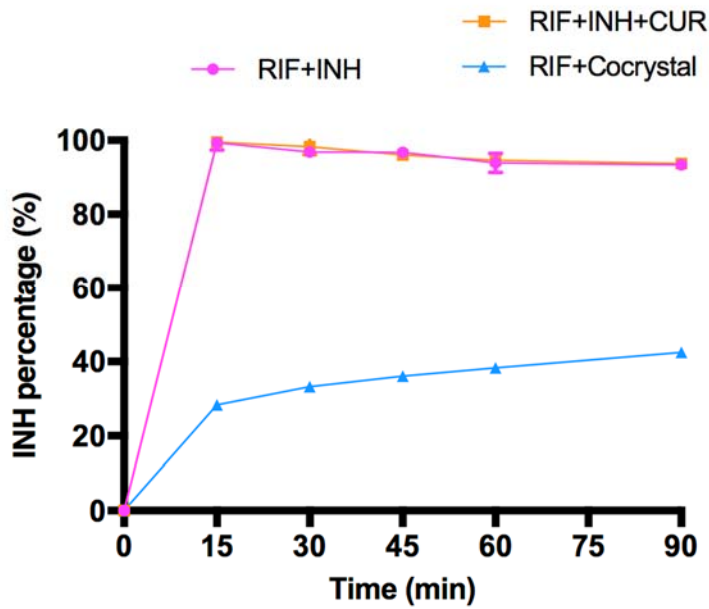
Figure 6. FTIR spectra of INH, CUR and 2:1 INH-CUR cocrystal.

1 (A)



2

3 (B)



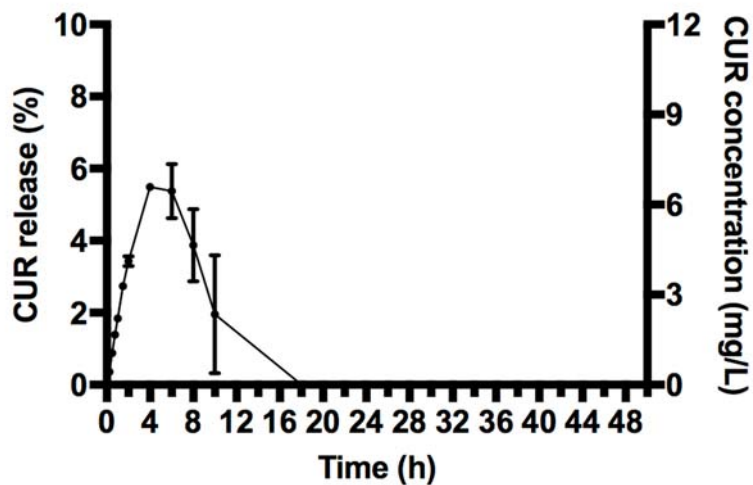
4

5 **Figure 7.** Dissolution profiles of RIF (A) and INH (B) from different sample groups in
6 pH 1.2 buffer solution (n=3).

7

8

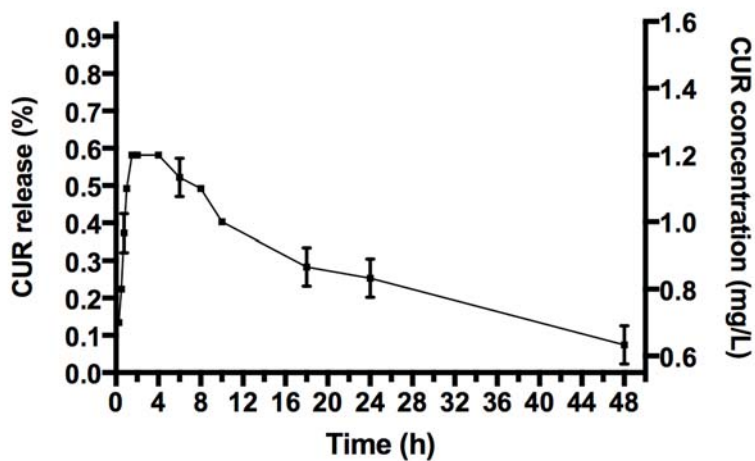
9 (A)



10

11 (B)

12

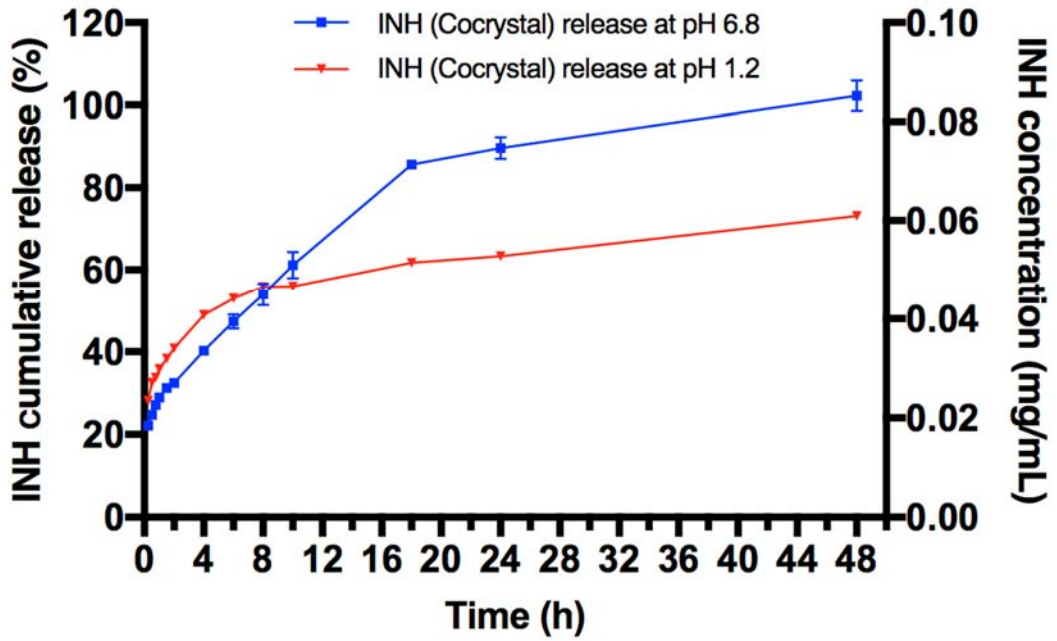


13

14

15 **Figure 8.** Dissolution profile of CUR from 2:1 INH-CUR cocrystal in the presence of
16 RIF in pH 1.2 (A) and pH 6.8 (B) buffer solutions (n=3).

17



18

19

20 **Figure 9.** Dissolution profile of INH from 2:1 INH-CUR cocrystal in the presence of RIF
 21 in pH 1.2 and pH 6.8 buffer solutions (n=3).

22

23

24

25

26

27

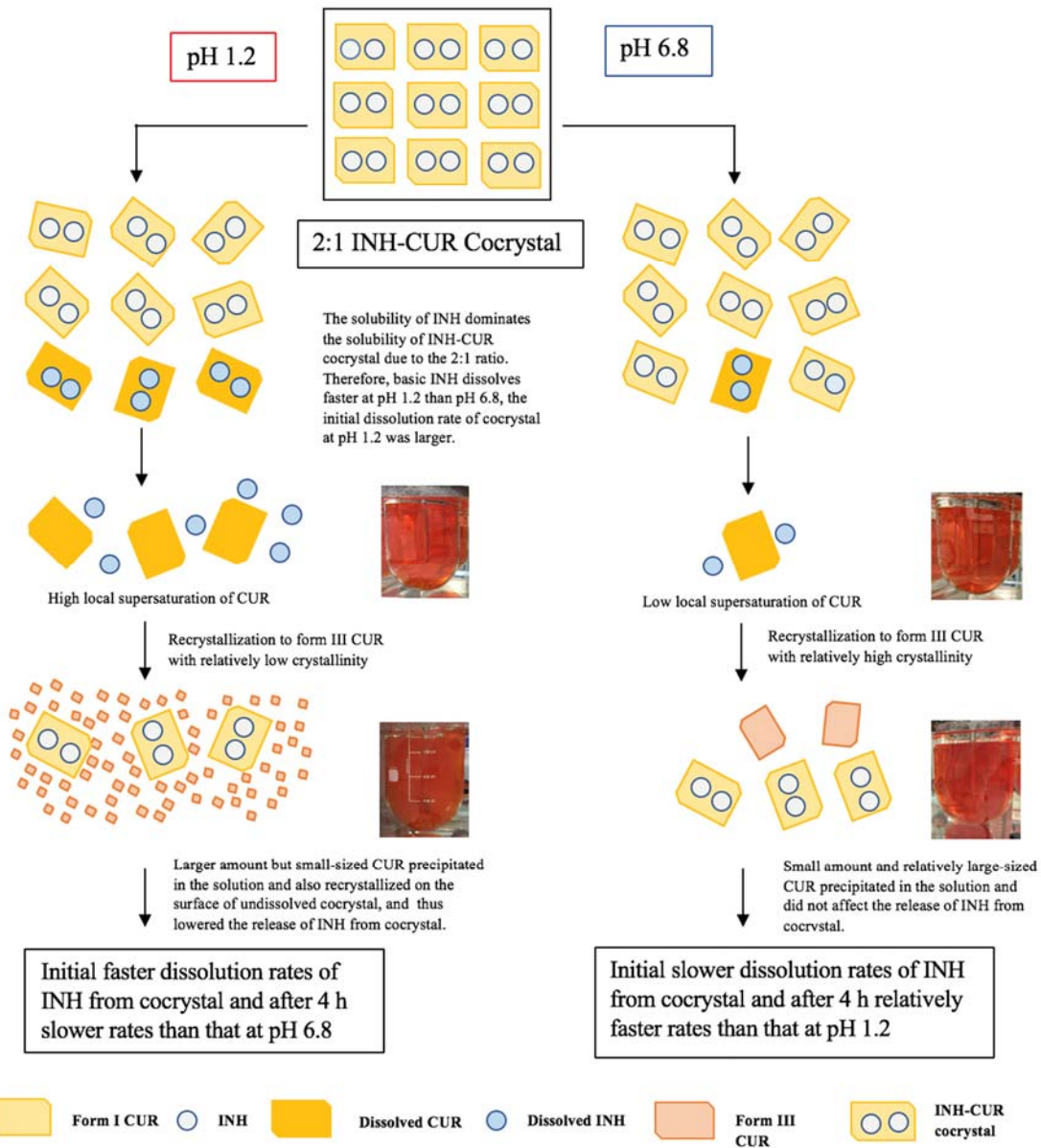
28

29

30

31

32



33
34
35
36
37
38
39
40

Figure 10. Proposed release mechanism of INH-CUR cocrystal at pH 1.2 and 6.8.

41 For Table of Contents Use Only,

42

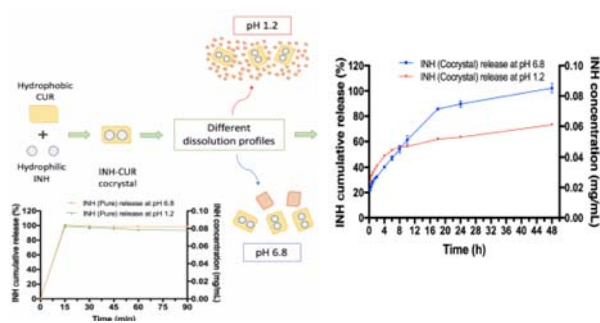
43 **Extended release of highly water soluble isoniazid attained through cocrystallization**
44 **with curcumin**

45 Bianfei Xuan¹, Si Nga Wong¹, Yanjie Zhang^{1,2}, Jingwen Weng¹, Henry Hoi Yee Tong³,

46 Chenguang Wang⁴, Changquan Calvin Sun⁴, Shing Fung Chow^{1,*}

47

48 TOC graphic:



49

50

51

52 Synopsis:

53 A new 2:1 isoniazid and curcumin cocrystal was prepared and characterized by PXRD,

54 DSC, temperature-composition phase diagram and FTIR. Extended release of hydrophilic

55 INH from the cocrystal was observed at pH 1.2 and pH 6.8. This work demonstrated that

56 cocrystallization is a promising formulation strategy for achieving up to 48 h of drug

57 release without using polymers.

58

59

60